Economic Dispatch of Electrolytic Copper Loads in Demand Response under Thermally-Enhanced RTN

Haocong XIE, Siyang LIAO*, Jian XU, *Senior Member, IEEE*, Deping KE, *Member, IEEE*, Lingfang LI,
Hubei Engineering and Technology Research Center for AC/DC Intelligent Distribution Network, School of Electrical Engineering and Automation, Wuhan University, Wuhan 430072, China

***Abstract*—The participation of Process Industrial Loads (PILs) in Demand Response (DR) is a key pathway to enhancing power system flexibility. However, existing dispatch models commonly treat core PIL production stages as "black-boxes," whose neglect of critical internal thermodynamic dynamics often leads to physically infeasible dispatch decisions. Concurrently, the lack of a fine-grained modeling method for PIL's power regulation costs presents another key barrier to their effective participation. To address these dual challenges, this paper, taking an Electrolytic Copper Load (ECL) as an example, first establishes a Thermally-Enhanced Resource-Task Network (ThE-RTN) to ensure the safety and feasibility of the dispatch plan. Subsequently, a fine-grained cost model that distinguishes different regulation modes is developed, and an economic dispatch model aimed at minimizing the total dispatch cost is formulated. A case study based on a real-world ECL demonstrates that the proposed framework can achieve economic optimality of the dispatch plan while satisfying both DR and production safety constraints, providing an effective solution for PILs to participate in grid interactions safely and economically.**

***Index Terms*—Demand Response(DR), Thermally-Enhanced Resource-Task Network (ThE-RTN), Economic Dispatch, Electrolytic Copper Load(ECL).**

I. INTRODUCTION

The "dual-carbon" goals are driving the development of a new-generation power system dominated by renewables, whose volatility, however, poses severe flexibility challenges [1]. Engaging demand-side resources in Demand Response(DR) is considered an economical and efficient way to enhance system flexibility[2]. In this context, industrial loads are regarded as ideal DR resources due to their high energy consumption, strong controllability, and willingness to participate[3],[4]. Their participation is of great significance for promoting the green development of the power industry and achieving the "dual-carbon" targets[5].

Aggregating and coordinating dispatchable stages of a Process Industrial Load (PIL) for DR participation requires fine-grained modeling of its production process, which often involves complex inter-stage material interactions and internal thermo-chemical reactions. To systematically describe its operational status, process modeling methods like the Resource-Task Network (RTN) and State-Task Network (STN) have been proposed[6],[7]. However, these models typically treat the core production stages of a PIL as "black-boxes," focusing on its macroscopic power regulation capability or inter-stage material balances, while systematically neglecting the critical intra-stage thermodynamic couplings among power, temperature, and efficiency. Dispatch plans based on such models may consequently be physically infeasible or even violate production safety constraints.

Economic benefit is the core driver for PILs to participate in DR, which involves power regulation decisions for dispatchable stages. However, most existing research focuses on the overall economic dispatch of industrial loads, with insufficient investigation into accurately modeling the regulation costs of individual stages and achieving economic optimality through multi-stage coordination. Therefore, determining an economic-optimal power allocation strategy while strictly adhering to the PIL's internal rigid production constraints is a key challenge that needs to be addressed for its effective participation in DR.

To address the dual challenges in modeling and economics, this paper proposes a power regulation strategy for a typical PIL, an Electrolytic Copper Load (ECL), in DR based on a Thermally-Enhanced Resource-Task Network. The main contributions are as follows:

i) A Thermally-Enhanced Resource-Task Network (ThE-RTN) model is proposed, which embeds the internal thermodynamic dynamics of electrolytic cells into the conventional RTN framework. This approach overcomes the limitations of "black-box" modeling and captures the relationship between intra-stage thermodynamic balance and inter-stage material interactions.

ii) A fine-grained method for calculating power regulation costs is developed, considering the continuous modulation and discrete start-stop characteristics of PIL stages. Based on this, an economic-optimal power allocation strategy is proposed, which co-optimizes DR requirements with the load's normal production order.

II. THERMALLY-ENHANCED MODELING OF THE ELECTROLYTIC COPPER LOAD

A. ECL Process Flow and Dispatchability Analysis

The ECL is a typical PIL, comprising several production stages: Material Preparation (MP), Side-blown Smelting (SBS), Top-blown Smelting (TBS), Anode Furnace Smelting (AFS), Casting (C), Electrolytic Refining (ER), Oxygen Production (OP), Auxiliary Smelting (AS), and Acid Production (AP). The MP stage supplies raw materials for subsequent processes. The pyrometallurgical stages (SBS, TBS, AFS) sequentially refine the material, while the C stage cools the molten anode copper. The OP and AS stages support the pyrometallurgical process by supplying oxygen-rich air, the AP stage produces acid from flue gas, and the ER stage electrolyzes anode copper to produce the final cathode copper product. A critical operational constraint is that the intermediate products of the pyrometallurgical stages are in a molten state, meaning they cannot be stored or exchanged with equipment on parallel production

979-8-3315-8138-1

This work was supported by the National Key Research and Development Program of China (No. 2023YFB2407300).

lines. [8] derived the coupling relationship between the power consumption and core production parameters of these stages, and identified stages such as MP, ER, and OP as being power-controllable. The power of controllable stages can be regulated through two primary means: continuous power modulation and discrete load switching. The power expression for a production unit is formulated as in Eq. (1):

$$P_{k,i}^{t} = P_{k,i}^{\text{rate},t} x_{k,i}^{t} s_{k,i}^{t} = P_{k,i}^{\text{rate},i} y_{k,i}^{t} \tag{1}$$

where $P_{k,i}^{t}$, $x_{k,i}^{t}$ and $s_{k,i}^{t}$ are the power consumption, regulation state, and binary commitment status (1=online) of unit i in stage k, respectively. $P_{k,i}^{\text{rate}}$ is the rated power. The state $x_{k,i}^{t}$ corresponds to key operational parameters subject to regulation boundaries ($\underline{x}_{k,i}$, $\overline{x}_{k,i}$) and is assumed constant over period t. Eq. (2) defines the specific regulation constraints:

$$\begin{cases} \underline{x}_{k,i} \le x_{k,i}^{t} \le \overline{x}_{k,i}, s_{k,i}^{t} \in \{0,1\} & k \in \{\text{MP},\text{ER}\} \\ \underline{x}_{k,i} \le x_{k,i}^{t} \le \overline{x}_{k,i}, s_{k,i}^{t} = 1 & k \in \{\text{PO},\text{PA},\text{AS}\} \\ x_{k,i}^{t} = s_{k,i}^{t} = 1 & k \in \{\text{SBS},\text{TBS},\text{AFS},\text{C}\} \end{cases} \tag{2}$$

The direct multiplication of a continuous variable $x_{k,i}^{t}$ and a binary variable $s_{k,i}^{t}$ as shown in Eq. (2) introduces a non-linear term that can cause computational challenges. Therefore, we employ the standard tight Big-M method to linearize this product. A new continuous variable, $y_{k,i}^{t}$ is introduced to represent the overall power regulation state of the production unit, which is governed by the constraint set (3):

$$\begin{cases} y_{k,i}^{t} \le \overline{x}_{k,i} s_{k,i}^{t} \\ y_{k,i}^{t} \le x_{k,i} - \underline{x}_{k,i}(1 - s_{k,i}^{t}) \\ y_{k,i}^{t} \ge x_{k,i}^{t} - \overline{x}_{k,i}(1 - s_{k,i}^{t}) \\ y_{k,i}^{t} \ge \underline{x}_{k,i} s_{k,i}^{t} \end{cases} \tag{3}$$

B. Formulation of the ThE-RTN Model

Based on the process characteristics of the ECL, it is established that the material interactions are constrained by the specific production lines of each stage. The material interaction dynamics over the production cycle are therefore formulated as shown in Eqs. (4)-(6):

$$R_{x}^{t} = R_{x}^{t-1} + \sum_{k}^{K} \sum_{i}^{n_k} v_{x,k,i} y_{k,i}^{t}, \forall x \in x_{\text{int}} \tag{4}$$

$$R_{x}^{t} = \sum_{i}^{n_k} (R_{x,i}^{t-1} + \sum_{k}^{K} v_{x,k,i} y_{k,i}^{t}), \forall x \in x_{\text{lim}} \tag{5}$$

$$\underline{R}_{x} \le R_{x}^{t} \le \overline{R}_{x}, \forall x \in \{x_{\text{int}}, x_{\text{lim}}\} \tag{6}$$

where R_{x}^{t} denotes the inventory of material x; and $v_{x,k,i}$ is the quantity produced/consumed by the i-th unit of stage k ($k \in$ K, $i \in n_k$). Inventory levels are constrained by safety stock and capacity limits ($\underline{R}_{x,i}$, $\overline{R}_{x,i}$). The interactions between materials and process stages are modeled as discrete-time events, which are assumed to occur only at the beginning or end of each time period. Fig. 1 depicts the material interaction network, modeled as discrete-time events.

For process stages possessing thermal inertia, their operational status is not solely determined by material interactions but is also strictly constrained by internal thermodynamics. In the ER stage, the electrolysis process must be conducted within a predefined electrolyte temperature range to ensure production safety. The electrolyte temperature is a critical state variable that influences the electrochemical reaction rate of cathode copper. Therefore, it is imperative to establish a dynamic model that characterizes the coupling relationship among power, temperature, and electrolytic efficiency. The temperature and boundary of the electrolyte in the discrete time period t can be expressed in Eq. (7)-(8):

$$T_{\text{ER},i}^{t} = T_{\text{ER},i}^{t-1} + \frac{\Delta t}{c_{\text{ER},i} m_{\text{ER},i}} (P_{\text{ER},i}^{\text{rate}} y_{\text{ER},i}^{t} x_{\text{heat}} - Q_{\text{ER},i}^{t}) \tag{7}$$

$$\underline{T}_{\text{ER},i} \le T_{\text{ER},i}^{t} \le \overline{T}_{\text{ER},i} \tag{8}$$

where $T_{\text{ER},i}$ is the temperature of electrolyte of the i-th electrolytic cell. Δt is the duration of a single time period, during which the heat dissipation power $Q_{\text{ER},i}$ is assumed to remain constant, justified by the strict and narrow operating temperature range of the electrolyte. x_{heat} is the efficiency of converting electrical energy into heat within the electrolytic cell. To ensure the proper progression of the electrolytic reaction, the electrolyte temperature must be maintained within its prescribed boundaries ($\underline{T}_{\text{ER},i}$, $\overline{T}_{\text{ER},i}$).

The deposition efficiency of cathode copper during the electrolytic reaction is significantly influenced by the temperature of the electrolyte[9]. This coupling relationship between electrolytic efficiency and electrolyte temperature is formulated as shown in Eq. (9):

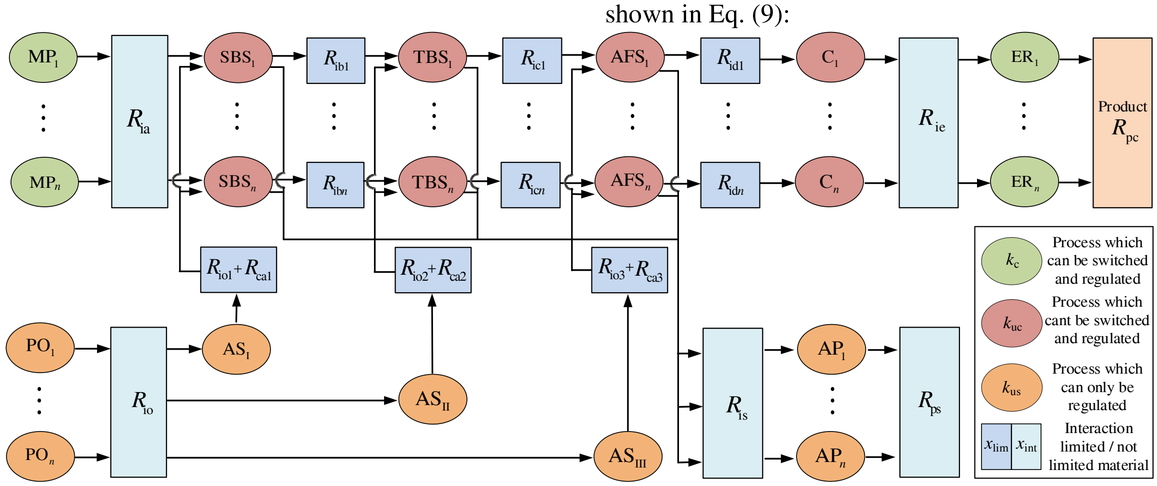

Fig. 1. Schematic of the material interaction network based on ECL process flow. R_{ia}, R_{ib}, R_{ic}, R_{id}, R_{ie}, R_{pc}, R_{io}, R_{ca}, R_{is}, R_{ps} represent raw material, liquid matte, liquid crude copper, liquid anode copper, solid anode copper, product cathode copper, oxygen, compressed air, sulfur-containing flue gas, sulfuric acid respectively. The character subscript represents the serial number of the corresponding production equipment. k_{c} represents process with power regulation feasibility. k_{uc} represents process without feasibility of power switching and regulation. k_{us} represents process without feasibility of power switching. x_{int} represents material that can interact between different production line. x_{lim} represents material whose interaction is limited to specific production line.

$$\eta_{\mathrm{ER},i} = \eta_{\mathrm{ER},i}^{\mathrm{rate}} - e_{\mathrm{ER},i}(T_{\mathrm{ER},i}^{\mathrm{rate}} - T_{\mathrm{ER},i}) \tag{9}$$

where $\eta_{\mathrm{ER},i}$ is the electrolytic efficiency of the i-th cell; $e_{\mathrm{ER},i}$ is the temperature-efficiency conversion coefficient; and $T_{\mathrm{ER},i}^{\mathrm{rate}}$ and $\eta_{\mathrm{ER},i}^{\mathrm{rate}}$ are the electrolyte temperature and the electrolytic efficiency of the i-th cell under rated operating conditions.

Based on the material balance principle established in Eq. (4), the cumulative inventory of the final product, cathode copper R_{pc} and production requirement can be formulated as Eq. (10)-(11):

$$R_{\mathrm{pc}}^{t} = R_{\mathrm{pc}}^{t-1} + \sum_{i}^{n_{\mathrm{ER}}} v_{R_{\mathrm{pc}},\mathrm{ER},i}\, y_{\mathrm{ER},i}^{t} \eta_{\mathrm{ER},i}^{t} \tag{10}$$

$$R_{\mathrm{pc}}^{T} - R_{\mathrm{pc}}^{0} \geq R_{\mathrm{aim}} \tag{11}$$

where R_{pc}^{T} and R_{pc}^{0} are the inventory levels of R_{pc} at the end and the beginning of the production cycle, respectively; and R_{aim} is the required production quantity for the entire production cycle.

From above, the effective production rate of cathode copper can be expressed as Eq. (12):

$$\begin{aligned} z_{\mathrm{ER},i}^{t} &= y_{\mathrm{ER},i}^{t} \eta_{\mathrm{ER},i}^{t} \\ &= \underbrace{[A_{\mathrm{ER},i} {y_{\mathrm{ER},i}^{t}}^{2} + F_{\mathrm{ER},i} y_{\mathrm{ER},i}^{t}]}_{\text{Part 1: SOS2, denoted as } f(y_{\mathrm{ER},i}^{t})} + \underbrace{E_{\mathrm{ER},i} \cdot T_{\mathrm{ER},i}^{t-1} \cdot y_{\mathrm{ER},i}^{t}}_{\text{Part 2: McCormick}} \end{aligned} \tag{12}$$

Eq. (12), with coefficients $A_{\mathrm{ER},i}$, $E_{\mathrm{ER},i}$, $F_{\mathrm{ER},i}$, renders the model a non-convex MINLP due to its quadratic (Part 1) and bilinear (Part 2) terms. To ensure solvability, we employ the Special Ordered Sets of Type 2 (SOS2) method[10] for the quadratic term and the McCormick relaxation[11] for the bilinear term.

To validate the approximation accuracy, we derive the theoretical upper bound of the total linearization error, denoted as $e_{\text{S-C}}$, which comprises the SOS2 interpolation error and the McCormick relaxation error:

$$e_{\text{S-C}} \leq \underbrace{\frac{1}{8} h^{2} \max |f''(y_{\mathrm{ER},i}^{t})|}_{\text{Part 1: } e_{\mathrm{SOS2}}} + \underbrace{\frac{1}{4} \Delta y_{\mathrm{ER},i}^{t} \Delta T_{\mathrm{ER},i}^{t}}_{\text{Part 2: } e_{\mathrm{McC}}} \tag{13}$$

Eq. (13) indicates that, benefiting from the narrow operating bands of the state variables($\Delta y_{\mathrm{ER},i}^{t}$,$\Delta T_{\mathrm{ER},i}^{t}$), this error bound is theoretically constrained to a negligible level, ensuring that the linearization preserves physical fidelity of the ThE-RTN model.

The aforementioned ThE-RTN model achieves aggregated and coordinated control of the different stages within the ECL's process flow. By considering both intra-stage and inter-stage production safety constraints when formulating dispatch plans, it provides a fundamental modeling basis for the ECL's participation in DR.

III. Formulation of the Economic-Optimal DR Dispatch Model for ECL

This section formulates a day-ahead economic dispatch model, which is executed after the DR market clearing. The objective is to optimize the production schedule within the DR period based on the confirmed response capacity.

A. Objective Function

The objective is to minimize the total dispatch cost F, which comprises continuous power regulation and discrete start-up/shut-down expenses, as in Eq. (14):

$$obj: \min F = \sum_{H=1}^{24} F_{\mathrm{cpr}}^{H} + F_{\mathrm{ud}}^{H} \tag{14}$$

where the time scale for H is one hour. The detailed modeling of the power regulation costs is presented in Eqs. (15)-(17):

$$F_{\mathrm{cpr}}^{H} = \sum_{t=4H-3}^{4H} \sum_{k}^{K} \sum_{i}^{n_k} (P_{k,i}^{\mathrm{rate}} \left|1 - y_{k,i}^{t}\right| \cdot \eta_{k,i}^{t}) \tag{15}$$

$$\eta_{k,i}^{t} = \begin{cases} \eta_{k,i}^{\mathrm{up}}, & 1 - y_{k,i}^{t} < 0 \\ \eta_{k,i}^{\mathrm{down}}, & 1 - y_{k,i}^{t} \geq 0 \end{cases} \tag{16}$$

$$F_{\mathrm{ud}}^{H} = \sum_{t=4H-3}^{4H} \sum_{k}^{K} \sum_{i}^{n_k} (u_{k,i}^{t} \eta_{k,i}^{\mathrm{su}} + d_{k,i}^{t} \eta_{k,i}^{\mathrm{sd}}) \tag{17}$$

where F_{cpr}^{H} and F_{ud}^{H} denote the continuous regulation and start-up/shut-down costs for hour H (with 15-min timescale t). $\eta_{k,i}^{t}$ denotes the unit regulation cost, determined by the specific upward/downward states($\eta_{k,i}^{\mathrm{up}}$, $\eta_{k,i}^{\mathrm{down}}$), while $\eta_{k,i}^{\mathrm{su}}$, $\eta_{k,i}^{\mathrm{sd}}$ and $u_{k,i}^{t}$, $d_{k,i}^{t}$ represent the corresponding single-action costs and binary statuses for start-up/shut-down. The regulation costs are calculated based on production costs within a maintenance cycle and relative weights determined via the Analytic Hierarchy Process (AHP)[8].

B. Constraints

To ensure the physical feasibility of the dispatch plan, the model must satisfy the following three core sets of constraints:

1)Production Safety Constraints

In perspective of production safety constraints, ECL must satisfy rigid production constraints at the power regulation, material, and thermodynamic levels. At the power regulation level, the constraints for stage equipment are defined in Eqs. (2)-(3). At the material level, the constraints for inter-stage material balance and final product quantity are given in Eqs. (4)-(6) and (9)-(11). At the thermodynamic level, the electrolyte temperature constraints are specified in Eqs. (7)-(8).

2)Stage Operational Logic Constraints

During power regulation, the start-up and shut-down status of the stage equipment must satisfy the constraints in (17)-(18). Specifically, constraint (19) ensures that a unit can either start up or shut down within the same time period t, but not both.

$$u_{k,i}^{t} - d_{k,i}^{t} = s_{k,i}^{t} - s_{k,i}^{t-1} \tag{18}$$

$$u_{k,i}^{t} + d_{k,i}^{t} \leq 1 \tag{19}$$

3)DR Requirement Constraints

The total period for the ECL's participation in DR is denoted as T_{r}. The required response capacity constraints are formulated in (20)-(22):

$$P_{\mathrm{ECL}}^{t_{\mathrm{r}}} = \sum_{k}^{K} \sum_{i}^{n_k} P_{k,i}^{\mathrm{rate}} y_{k,i}^{t_{\mathrm{r}}} \tag{20}$$

$$C_{\mathrm{res}}^{H_{\mathrm{r}}} = \sum_{t_{\mathrm{r}}=4H_{\mathrm{r}}-3}^{4H_{\mathrm{r}}} (P_{\mathrm{base}}^{t_{\mathrm{r}}} - P_{\mathrm{ECL}}^{t_{\mathrm{r}}}) \Delta t \tag{21}$$

$$C_{\mathrm{res}}^{H_{\mathrm{r}}} \geq C_{\mathrm{bid}}^{H_{\mathrm{r}}}, \forall H_{\mathrm{r}} \in T_{\mathrm{r}} \tag{22}$$

where $P_{\mathrm{ECL}}^{t_{\mathrm{r}}}$ and $P_{\mathrm{base}}^{t_{\mathrm{r}}}$ represent the ECL power and baseline power at DR time period t_{r}, respectively; $C_{\mathrm{res}}^{H_{\mathrm{r}}}$ and $C_{\mathrm{bid}}^{H_{\mathrm{r}}}$ are the actual and awarded response capacities for the H_{r}-th hour. The time scales for H_{r} and t_{r} are one hour and 15 minutes, respectively. Eq. (21) defines the actual response capacity as the sum of the power reduction from the baseline over the response period. Eq. (22) is the DR capacity constraint, which stipulates that the actual response capacity must not be lower than the awarded capacity. Furthermore, to ensure an effective DR, the peak and average values of the ECL actual power during the DR period must not exceed those of the baseline, as expressed in constraints (23)-(24):

$$P_{\mathrm{lmax}}^{H_{\mathrm{r}}} \leq P_{\mathrm{bmax}}^{H_{\mathrm{r}}}, \forall H_{\mathrm{r}} \in T_{\mathrm{r}} \tag{23}$$

$$P_{\mathrm{lav}}^{H_{\mathrm{r}}} \leq P_{\mathrm{bav}}^{H_{\mathrm{r}}}, \forall H_{\mathrm{r}} \in T_{\mathrm{r}} \tag{24}$$

where $P_{\mathrm{lmax}}^{H_{\mathrm{r}}}$ and $P_{\mathrm{lav}}^{H_{\mathrm{r}}}$ are the maximum and average power of the load during the response period H_{r}, respectively. $P_{\mathrm{bmax}}^{H_{\mathrm{r}}}$ and $P_{\mathrm{bav}}^{H_{\mathrm{r}}}$ are the corresponding maximum and average power values of the load baseline. These constraints ensure the quality of the demand response.

IV. Case Study

To validate the effectiveness of the proposed economic-optimal DR dispatch model for ECL, this section presents a comprehensive case study based on a typical ECL located in Yunnan, China. The entire optimization model is formulated using the YALMIP modeling language within the MATLAB R2023a environment and solved by the commercial solver Gurobi 12.0. The computations were performed on a personal computer equipped with an Intel Core i9-14900HX CPU and 32 GB of RAM. The scheduling cycle is discretized into 15-minute time periods, constituting a 24-hour production cycle with a total of 96 periods.

A. Parameter Settings

Validation is based on real-world ECL data, with stage and cost parameters detailed in Tables I and II. Key settings include: storage caps for materials(R_{ia}, R_{io}, R_{ca}, R_{is}) of 1500, 4800, 1500, and 60, with initial stocks of 1000 for R_{ia} and 2400 for R_{io}. A production target for R_{pc} within the production cycle is 7500. For the ER stage, the temperature is constrained to 35-40°C (initialized at 40/39.5/40°C), with a maximum efficiency of 0.99 and a conversion coefficient $e_{\mathrm{ER},i}$ of 0.01. The scenario simulates a day-ahead DR event (15:00-19:00) with awarded capacities of 10023, 23750, 9503, and 25787 kWh.

TABLE I Power Consumption And Regulation Boundaries of Production Stages of ECL

Process Flow	Power consumption (kWh/h)	Power regulation boundaries	
		Lower limit	Upper limit
MP	15793	0.85	1.05
SBS	16437	/	/
TBS	16437	/	/
AFS	10296	/	/
C	11100	/	/
ER (Set I)	21689	0.75	1.05
ER (Set II)	21689	0.75	1.05
ER (Set III)	21689	0.75	1.05
OP	45560	0.8	1.05
AS (Set I)	5356	0.95	1
AS (Set II)	4656	0.9	1
AS (Set III)	3456	0.8	1
AP	25902	0.9	1.05

979-8-3315-8138-1

TABLE II Power Regulation Cost of Production Equipment With Power Regulation Feasibility

Process Stage	MP Stage	ER Stage	OP Stage	AS Stage	AP Stage
Down (*yuan*/kWh)	0.2094	0.2944	0.2116	0.0346	0.3566
Up (*yuan*/kWh)	0.4188	0.5299	0.4232	0.0346	0.7132
Shut-Down (*yuan*/per time)	20	60	/	/	/
Start-up (*yuan*/per time)	10	40	/	/	/

B. Comparative Analysis: Economic Performance, Operational Feasibility, and Production Safety

To validate the necessity of the proposed framework, we compare the ThE-RTN with a conventional RTN model (which ignores thermodynamic constraints). The comparative results regarding dispatch costs, production targets, and safety constraints are presented in Table III and Figs. 2–4.

TABLE III Comparison of DR Response Performance and Dispatch Costs Between Models

Model	Response Capacity $C_{\mathrm{res}}^{H_{\mathrm{r}}}$ (kWh)				Dispatch Cost F (*yuan*)
	H_{r}=1	H_{r}=2	H_{r}=3	H_{r}=4	
Proposed ThE-RTN	10023	23750	9530	25787	9781.1
Conventional RTN	10023	23750	9530	25787	9737.6

As shown in Table III, the conventional RTN model appears to achieve a marginally lower dispatch cost. This is primarily because it prioritizes regulating the power-intensive electrolysis stage to minimize costs, as indicated by the regulation patterns in Fig. 2. However, a deeper analysis reveals that this economic advantage is a "false optimum" obtained by violating critical physical constraints.

First, regarding operational feasibility, Fig. 3 indicates that the conventional model fails to meet the rigid production demand, yielding only 7473 t of cathode copper against the 7500 t target (Fig. 3(b)). In contrast, the ThE-RTN successfully fulfills the quota (Fig. 3(a)). Second, and more critically regarding production safety, Fig. 4 exposes severe violations in the conventional schedule. As the model blindly reduces power, the electrolyte temperature drops significantly below the lower safety limit of 35°C (Fig. 4(b)), thereby severely compromising product quality and production safety. Conversely, the ThE-RTN maintains the temperature strictly within the safe range of 35-40°C (Fig. 4(a)).

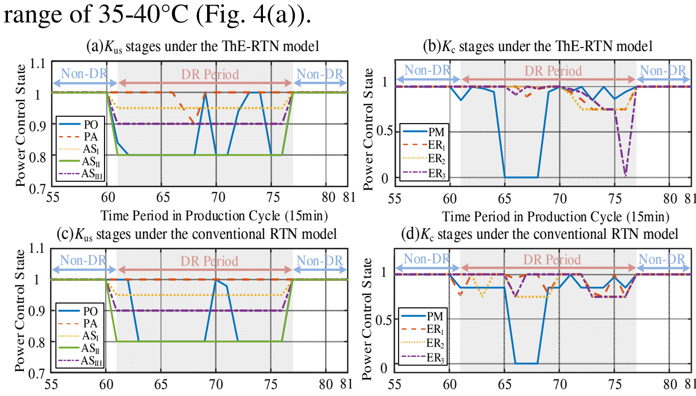

Fig. 2. Comparison of power regulation states. (a)-(b) Regulated states under ThE-RTN model; (c)-(d) Regulated states under conventional RTN model.

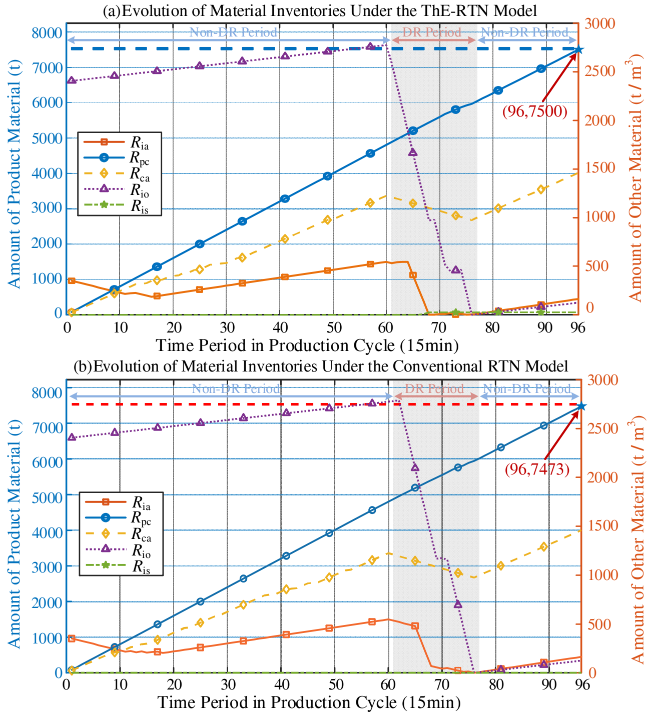

Fig. 3. Evolution of material inventories. (a)Evolution of material inventories under the ThE-RTN models; (b)Evolution of material inventories under the conventional RTN models.

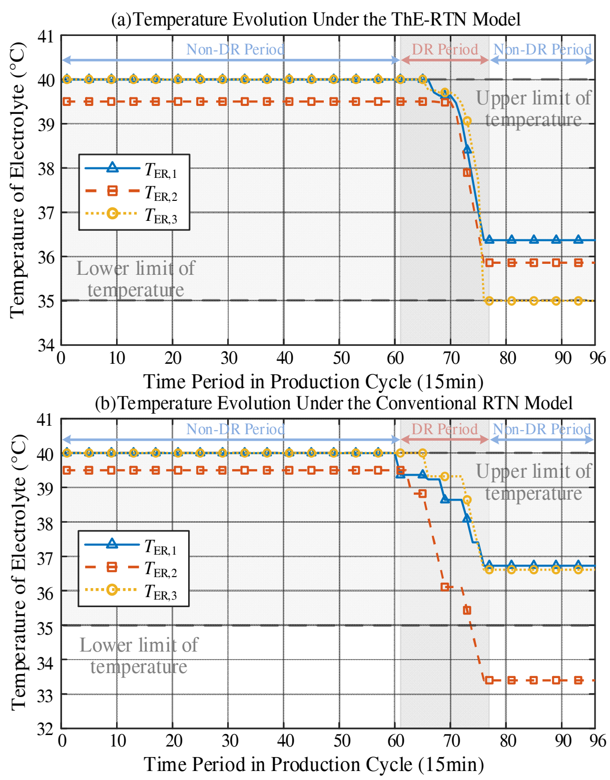

Fig. 4. Evolution of electrolyte temperatures. (a)Evolution of temperatures under the ThE-RTN RTN models; (b)Evolution of temperatures under the conventional RTN models.

In summary, the comparative results validate that the proposed ThE-RTN framework effectively navigates the trade-off between economy and safety. By incorporating thermodynamic constraints, it produces a dispatch plan that is not only economically optimized under real-world conditions but, more importantly, operationally feasible and safe, all while precisely meeting the grid's DR requirements.

C. Algorithm Accuracy and Solution Sensitivity

This section evaluates the linearization accuracy and model robustness. Computationally, the model achieves a global optimum within 0.62 s, with a negligible optimality gap of 0.0098%. The resulting schedule yields an actual production of 7491.4 t, with a relative linearization error of only 0.1146%. This deviation satisfies the theoretical upper bound derived in Eq. (13), confirming that the linearization error is negligible. Furthermore, sensitivity analysis shows that a 20% increase in power regulation costs leads to a proportional total cost rise to 11,737 (also a 20% increase). This indicates that the optimal dispatch strategy remains highly stable against economic parameter fluctuations.

V. Conclusion

This paper proposes an economic dispatch model based on the ThE-RTN to address the dual challenges of production safety and economic efficiency when PILs participate in DR. Using an ECL as an example, the model embeds thermodynamic balance into the conventional RTN and incorporates fine-grained regulation costs to establish the optimal dispatch model. Simulation results demonstrate that the proposed strategy minimizes total dispatch costs while strictly adhering to production safety and DR constraints. Finally, the proposed framework exhibits significant transferability to other energy-intensive industries (e.g., steel, aluminum), as the key flexible stages—specifically motor-driven material preparation and electrolysis processes—are generic and widely applied across various industrial loads.

References

[1] H. Golmohamadi, "Demand-side management in Industrial Sector: A review of Heavy Industries", *Renewable and Sustain. Energy Rev.*, vol. 156, pp. 111963, 2022.

[2] B. Mohandes, M. S. El Moursi, N. D. Hatziargyriou, and S. El Khatib, "Incentive based demand response program for power system flexibility enhancement," *IEEE Trans. Smart Grid*, vol. 12, no. 3, pp. 2212-2223, May, 2021.

[3] H. Golmohamadi, "Demand-side management in industrial sector: A review of heavy industries," *Renewable and Sustainable Energy Reviews*, vol. 156, p. 111963, Mar. 2022.

[4] P. Bao, W. Zhang and Y. Zhang, "Secondary frequency control considering optimized power support from virtual power plant containing aluminum smelter loads through VSC-HVDC link", *J. Mod. Power Syst. Clean Energy*, vol. 11, no. 1, pp. 355-367, Jan. 2023.

[5] B. Williams, D. Bishop, P. Gallardo, and J. G. Chase, "Demand side management in industrial, commercial, and residential sectors: A review of constraints and considerations," *Energies*, vol. 16, no. 13, p. 5155, Jul. 2023.

[6] Y. M. Ding, S. H. Hong and X. H. Li, "A demand response energy management scheme for industrial facilities in smart grid," *IEEE Trans. Ind. Inform.*, vol. 10, no. 4, pp. 2257-2269, Nov. 2014.

[7] H. Wang, L. Zhang, "Supply-demand interactive scheduling model considering short production process of steel enterprises," *Automation of Electric Power Syst.*, vol. 45, pp. 64-76, 2021.

[8] S. Liao, H. Xei, J. Xu, et al. "Demand Response Control Strategy for High-energy-consuming Loads Aligned With Demand-side Market Response Transaction Rules," *Proceedings of the CSEE*. vol. 45, no. 5, pp. 1645-1657, 2025.

[9] Y. Sun, B. Ren, H. Wang et al. "Effect of Process Conditions on Power Consumption of Copper Electrorefining," *NONFERROUS METALS(EXTRACTIVE METALLURGY)*, vol. 6, pp. 5-8, 2018.

[10]Zheng C, Fang J, Wang S, et al. "Energy flow optimization of integrated gas and power systems in continuous time and space," *IEEE Transactions on Smart Grid*, vol. 12, no. 3, pp. 2611-2624, 2020.

[11]ROSENBLATT M. "Remarks on some nonparametric estimates of a density function. *Annuals of Mathematical Statistics*," vol. 27, no. 3, pp. 832-837,1965.